J. Min. Metall. Sect. B-Metall. 62 (2) (2026) 177 - 193

Journal of Mining and Metallurgy, Section B: Metallurgy

INTERFACE INTERACTION BETWEEN COMPLEX OXIDES AND THE MATRIX OF Si-Mn DEOXIDIZED STEEL DURING HEAT TREATMENT

Xinlong Nie [a], Shannan Li [a], Qi Xu [a], Jianli Li [a,b,c,*]

[a] Key Laboratory for Ferrous Metallurgy and Resources Utilization of Ministry of Education, Wuhan University of Science and Technology, Wuhan, Hubei, China
[b] Hubei Provincial Key Laboratory for New Processes of Ironmaking and Steelmaking, Wuhan University of Science and Technology, Wuhan, Hubei, China
[c] National Key Laboratory of Advanced Refractory Materials, Wuhan, Hubei, China

(Received 01 April 2026; accepted 23 June 2026)

Abstract

Diffusion couples were prepared using a high-temperature furnace to investigate the interfacial reactions between Si-Mn deoxidized steel and $CaO-SiO_2-Al_2O_3-MgO-MnO$ / $CaO-SiO_2-Al_2O_3-MgO-MnO-FeO$ oxide systems during heat treatment at 1273, 1373, and 1473 K for 10 hours. The effects of these reactions on the composition and phase evolution at the interface were systematically examined. Furthermore, the influence of FeO content and varying heat treatment temperature on the interfacial behavior between complex oxides and the Si-Mn deoxidized steel substrate was explored. The results indicate that, regardless of the initial FeO content in the oxide phase of the diffusion couples, precipitates consisting of SiO_2 and a small amount of MnO formed in the steel matrix after heat treatment. Near the interface, a dark phase with a high SiO_2 content precipitated in the oxide. The widths of the manganese-depleted zone (MDZ) and the particle precipitation zone (PPZ) were found to be approximately linearly correlated. Compared with the FeO-free system, diffusion couples containing 3 wt% FeO exhibited broader MDZ and PPZ in the steel matrix after heat treatment. The maximum widths of both the MDZ and PPZ were observed under the heat treatment condition of 1373 K for 10 hours.

Keywords: *Diffusion couple; Si-Mn deoxidized steel; Complex oxide; Interfacial reaction; Heat treatment*

1. Introduction

Non-metallic inclusions play a critical role in determining the quality of steel products, making their study a key focus in this field. Numerous studies have investigated the behavior of non-metallic inclusions in molten steel and during solidification. However, the final quality of steel products is often determined by the state of these inclusions after heat treatment and mechanical processing. It has been reported that the inclusions present in steel after heat treatment and rolling often differ significantly from the initial inclusions in the molten steel before solidification. The influence of heat treatment processes on the physicochemical properties of non-metallic inclusions in steel has attracted extensive research attention [1-6].

Due to their relatively low hardness and melting point, Si-Mn deoxidation products exhibit high deformability during the rolling process. As a result, Si-Mn deoxidized steel is widely used in the production of spring steel and cord steel owing to its excellent processability, which helps avoid the formation of Al_2O_3-type inclusions typically associated with aluminum deoxidation [7-10]. However, after the heat treatment, the composition of non-metallic inclusions changes significantly. This transformation is primarily attributed to interfacial reactions between the steel matrix and the inclusions during heat treatment [10-17]. These reactions alter the properties of the original inclusions and promote the precipitation of new inclusions. This leads to a decrease in the manganese content in the alloy in the region near the interface between the steel matrix and the oxide inclusions, resulting in the formation of a "manganese-depleted zone". The presence of a manganese-depleted zone reduces the stability of austenite and increases the driving force for ferrite nucleation. This promotes intragranular ferrite (IGF) nucleation, thereby contributing to grain refinement and improving the strength and toughness of the steel [10-12, 18-24]. Therefore, investigating and optimizing appropriate heat treatment processes is of significant importance for enhancing the mechanical properties and overall quality of steel.

Kim et al. [25] investigated the effect of sulfur on

Corresponding author: jli@wust.edu.cn

https://doi.org/10.2298/JMMB260401014N

the reaction between MnO-SiO_2-FeO oxides and a Fe-Mn-Si alloy. The results demonstrate that at a heat treatment temperature of 1473 K, the widths of the particle precipitation zone (PPZ) and the manganese-depleted zone (MDZ) in the alloy decreased significantly with increasing sulfur content in the oxide and decreasing sulfur content in the steel matrix. Furthermore, under the same heat treatment conditions, the mass fraction of MnS in the oxide also exhibited a decreasing trend. Zhang et al. [26] investigated the solid-state reaction between MnO-SiO_2-FeO oxides and a silicon-manganese deoxidized steel matrix at 1473 K. The results indicate that during heat treatment, fine oxide particles precipitated in the alloy, and the widths of the particle precipitation zone (PPZ) and the manganese-depleted zone (MDZ) gradually increased with prolonged heat treatment time. During the 0-20 h heat treatment period, particularly within the initial 0-5 h, significant decomposition of FeO in the oxide occurred, leading to a rapid increase in the widths of the manganese-depleted zone (MDZ) and the particle precipitation zone (PPZ). As the heat treatment duration was extended to 30-50 h, the solid-state reaction between the oxide and the alloy at the interface was gradually suppressed, resulting in a noticeable deceleration in the growth rate of both the MDZ and PPZ widths. Liu et al. [23] investigated the effects of FeO and sulfur on the solid-state reaction between MnO-SiO_2-FeO oxide and Fe-Mn-Si alloy. The results showed that as the sulfur content in the oxide increased, the diffusion of oxygen into the steel matrix was inhibited, reducing the widths of the particle precipitation zone (PPZ) and the manganese-depleted zone (MDZ). Meanwhile, the mass fraction of MnS in the oxide exhibited a decreasing trend at 1473 K. When the FeO content in the oxide decreased, the interfacial reaction could still occur; however, high sulfur content effectively suppressed the precipitation and growth of inclusions. Wang et al. [27] investigated the interactions of Al_2O_3 and MgO with a low-density steel during heat treatment at 1373 K for 10 hours. It was found that oxygen diffused from these oxides into the steel matrix, leading to the formation of a particle precipitation zone (PPZ). This process resulted in morphological changes in non-metallic inclusions, such as the spheroidization of MnS, an increase in the number of fine AlN inclusions, and the diffusion of manganese towards the interface. These changes help to improve the internal structure and uniformity of the steel, thereby improving the overall performance of the material. The aforementioned studies indicate that the composition and morphology of non-metallic inclusions in steel can be modified through appropriate heat treatment processes. Factors such as temperature, time, and the presence of elements like FeO and sulfur in the inclusions or at the interface can significantly influence the steel-inclusion reactions, thereby affecting the final inclusion characteristics and improving the properties of the steel [23]. However, previous research has not extensively explored the influence of different heat treatment temperatures on the interfacial behavior between complex oxides and Si-Mn deoxidized steel matrix. Moreover, the effect of FeO content in complex oxides under varying heat treatment temperatures on such interfacial interactions remains insufficiently studied. Additionally, most existing literature on Si-Mn deoxidized steel and non-metallic inclusions has primarily focused on ternary systems. In this study, diffusion couples were prepared by bonding Si-Mn deoxidized steel substrates with CaO-SiO_2-Al_2O_3-MgO-MnO and CaO-SiO_2-Al_2O_3-MgO-MnO-FeO oxides using a high-temperature furnace. The couples were isothermally heat-treated at temperatures ranging from 1273 to 1473 K for 10 hours to investigate the effects of heat treatment temperature and FeO content on the interfacial behavior between the complex oxides and the Si-Mn deoxidized steel matrix. The purpose of this study is to investigate the interfacial reaction mechanism between Si-Mn deoxidized steel and inclusions under optimal heat treatment conditions, and to elucidate its regulatory effect on inclusion composition and its influence on the distribution of manganese and silicon in the steel matrix. This research aims to provide a theoretical basis for optimizing the comprehensive performance and quality of steel, and therefore holds significant research value.

2. Experimental methods

The compositions of the alloys and oxides selected in this study are listed in Table 1 and Table 2, respectively. The steel used was LX82A Si-Mn deoxidized billet. Its chemical composition was determined by sampling molten steel from the tundish and analyzing it via optical emission spectrometry, with an oxygen content of 11 ppm measured in the steel. The oxide composition is based on the average composition of oxide inclusions in LX82A Si-Mn deoxidized billet before heat treatment measured in previous work [28]. To investigate the effect of FeO on the interface between the steel matrix and the oxide, an additional oxide containing 3 wt.% FeO was prepared. The FeO content was determined based on the high-temperature equilibrium composition between the alloy and the oxide at 1873 K. The melting points of both oxides were calculated using FactSage 8.0 software. The results showed that the melting point of the oxide without FeO was 1667 K, while that containing 3 wt.% FeO was 1637 K.

(i) Diffusion couple production experiment. To achieve effective bonding between the LX82A Si-Mn

Table 1. *Chemical composition (mass fraction / %) of LX82A Si-Mn deoxidized steel*

C	Si	Mn	P	S	Cr	Ni	Mo	Cu	Al
0.813	0.18	0.511	0.014	0.011	0.035	0.011	0.0017	0.024	0.0012

Table 2. *Composition of composite oxides used in the experiment (mass fraction / %)*

CaO	SiO_2	Al_2O_3	MgO	MnO	FeO
13.27	66.45	12.77	5.93	1.58	0
12.86	64.5	12.38	5.74	1.52	3

deoxidized steel matrix and the oxide, the oxide was first pre-melted using a high-temperature tube furnace. The specific procedure was as follows: A sample of Si-Mn deoxidized steel LX82A was sectioned from a continuous casting billet into dimensions of 15 mm × 10 mm × 15 mm. A hole with a diameter of 3 mm was drilled on the surface of the steel block to accommodate the oxide particles. The prepared sample was then placed in a high-temperature furnace and heated from room temperature to 50 K above the melting point of the oxide. After holding at this temperature for 15 minutes to ensure complete and homogeneous melting of the oxide, the sample was rapidly removed from the furnace and cooled ambiently to room temperature. Prior to the heat treatment experiments, each diffusion couple was mounted, ground, polished, and coated with a thin layer of gold. The back scattering mode (BSE) of a field emission scanning electron microscope (SEM, Zeiss-EVO MA10) was used to observe the interface morphology, and the composition at the interface was detected and recorded by a matching energy spectrum analyzer. The diffusion couple samples without FeO and scheduled for heat treatment at 1273 K, 1373 K, and 1473 K were designated as A0-0, A1-0, and A2-0, respectively, while those containing FeO were designated as B0-0, B1-0, and B2-0, respectively.

(ii) Heat treatment experiment and sample analysis. The heat treatment temperatures in this experiment were set to 1273 K, 1373 K, and 1473 K, with a holding time of 10 hours. The samples were heated to the specified temperatures at a g rate of 300K / min, and the oxide pre-melting device and heat treatment test process are shown in Fig.1. A vertical resistance furnace was selected for heat treatment, as shown in Fig.2 (a). It is mainly composed of a heating system, temperature control system, thermal insulation structure, external protective gas system, and cooling water system. The equipment has good temperature uniformity and stability, and is suitable for high temperature heat treatment experiments. During the heat treatment process, the samples were not heated with the furnace from room temperature. Instead, they were inserted into the high-temperature furnace only after it had reached the designated soaking temperature. Furthermore, to avoid potential oxide defects induced by water quenching and to maximally suppress internal reactions that might occur during cooling, the cooling stages following both the oxide pre-melting and the heat treatment experiments were conducted by air cooling (removing the samples from the furnace and cooling them in ambient air).

The diffusion couple sample after pre-melting is shown in Figure 2 (b). The oxide is bonded to the steel matrix. After the heat treatment is completed, it is inlaid into the sample. After grinding, polishing, and gold spraying, the oxide and the steel matrix boundary line is taken as the center. The vertical line is made, and the SEM-EDS point analysis is used to detect the points along the straight line interval. The measured contents of Ca, Si, Al, Mg, Mn, and Fe were directly converted into mass fractions of their respective oxides, namely CaO, SiO_2, Al_2O_3, MgO, MnO, and FeO [14]. The diffusion couple samples without FeO heat-treated at 1273 K, 1373 K, and 1473 K were designated as A0-10, A1-10, and A2-10, respectively, while those containing FeO were labeled as B0-10, B1-10, and B2-10, respectively. The obtained results were analyzed to investigate the effects of heat treatment and FeO content on the interaction mechanisms between complex oxides and the silicon-manganese deoxidized steel substrate.

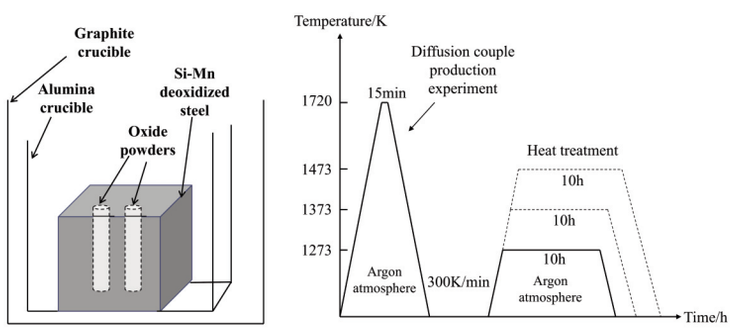

Figure 1. *Oxide pre-melting experimental device and heat treatment experimental temperature curve*

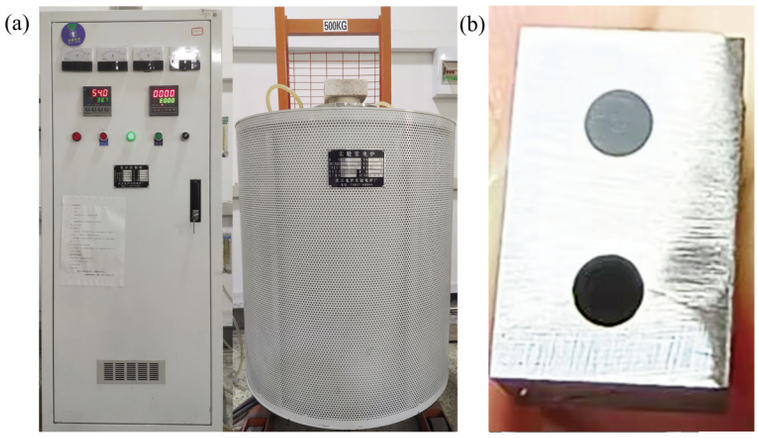

Figure 2. *Vertical resistance furnace (a) and diffusion couple sample (b)*

3. Results

3.1. Interface morphology of alloy and oxide

Figure 3 shows the interfacial morphology between Si-Mn deoxidized steel and the CaO-SiO_2-Al_2O_3-MgO-MnO oxide before heat treatment and after 10 hours of heat treatment at 1273 K, 1373 K, and 1473 K. As shown in Figure 3(a), (b), and (c), after the oxide premelting experiment, the interfaces between the Si-Mn deoxidized steel matrix and the oxide exhibit good bonding in all samples. The oxides are homogeneous, and no precipitated particles are observed in the steel matrix. Following heat treatment, the formation of new phases is observed at the interface in samples A0-10, A1-10, and A2-10, along with the precipitation of fine black particles in the adjacent steel matrix. As the heat treatment temperature increases, the number of these precipitates within the steel matrix continues to rise. In sample A0-10, a certain amount of elongated and fine particulate precipitates formed in the steel matrix near the interface. After the diffusion couple was heat-treated at 1373 K for 10 hours, elongated precipitates composed of fine particles were observed in the steel matrix of sample A1-10. Compared to A0-10, the particulate precipitates near the interface exhibited an increase in size, while those approximately 10 μm away from the interface showed a decrease in size. When the heat treatment temperature was further increased to 1473 K, the number of particulate precipitates near the interface in sample A2-10 further increased, and no elongated precipitates were observed. After heat treatment, black and gray phases were present in the oxides of samples A0-10, A1-10, and A2-10.

The interfacial compositions of the samples (A0-0, A0-10, A1-0, A1-10, A2-0, and A2-10) were analyzed using SEM-EDS, and the results are presented in Table 3-8. Since the oxide in the diffusion couple samples was homogeneous and no precipitates were present in the steel matrix before heat treatment, only the oxide compositions near the interface in samples A0-0, A1-0, and A2-0 were examined. As shown in Tables 3, 5, and 7, although the initial composition of the oxide did not contain FeO, a small amount of FeO was detected in the oxide near the interface of samples A0-0, A1-0, and A2-0 after the diffusion couple fabrication process (i.e., after oxide premelting and before the heat treatment experiment). As shown in Tables 3 and 4, after the diffusion couple sample A0-0 was heat-treated at 1273 K for 10 h, the mass fractions of various components in the oxide near the interface exhibited some fluctuations. For example, the mass fraction of Al_2O_3 increased by approximately 1%. However, the overall composition of the oxide showed no significant changes. In addition, the elongated precipitates formed in the steel matrix were identified primarily as SiO_2, with a mass fraction exceeding 90%, along with minor amounts of CaO and MnO. As shown in Tables 5 and 6, the composition of the dark phase oxide near the interface of sample A1-10 exhibits varying degrees of mass fraction fluctuation compared to sample A1-0 before heat treatment: the mass fraction of SiO_2 increased, while those of MgO, CaO, and MnO decreased. In addition, the mass fractions of MgO and CaO in the grey phase oxide increased, while those of Al_2O_3 and FeO decreased. Granular precipitates in the steel matrix were found to consist mainly of SiO_2 and MnO. When the heat treatment temperature was increased to 1473 K, the oxide at the interface of sample A2-10 was observed to be primarily composed of a gray phase, accompanied by some attached dark phase. As shown in Tables 7 and 8, compared with sample A2-0 before heat treatment, the gray phase oxide near the interface of A2-10 exhibits a decrease in the mass fraction of MnO and an increase in that of FeO. The dark phase oxide at locations 4, 5, and 6 near the interface had a high SiO_2 content, with an average mass fraction of approximately 95%, and

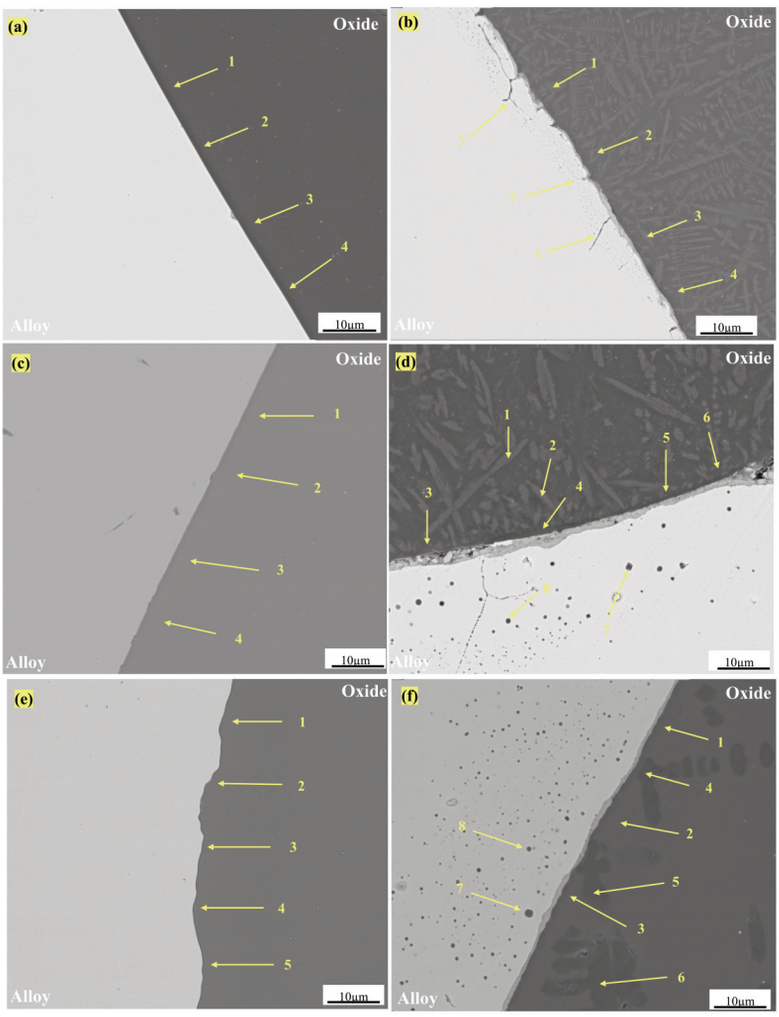

Figure 3. *The interface morphology between Si-Mn deoxidized steel and CaO-SiO_2-Al_2O_3-MgO-MnO oxide before heat treatment and after heat treatment at 1273 K, 1373 K and 1473 K for 10 h: (a) A0-0; (b) A0-10; (c) A1-0; (d) A1-10; (e) A2-0; (f) A2-10*

Table 3. *Chemical composition (mass fraction / %) at each position in diffusion couple A0-0*

position	MgO	Al_2O_3	SiO_2	CaO	MnO	FeO
1	4.67	11.57	67.34	12.36	1.53	2.53
2	4.8	11.27	67	12.27	1.51	3.15
3	5.11	11.37	65.95	11.54	1.85	4.18
4	5.25	11.49	66.56	11.79	1.73	3.19

Table 4. *Chemical composition (mass fraction / %) of each position in diffusion couple A0-10*

position	MgO	Al_2O_3	SiO_2	CaO	MnO	FeO
1	4.22	12.62	67.98	11.44	1.81	1.94
2	4.8	12.31	66.74	12.36	1.59	2.2
3	4.52	12.28	67.56	11.97	1.56	2.12
4	3.49	12.68	68.86	11.22	1.82	1.93
5	/	/	96.44	1.65	1.9	/
6	0.05	/	98.59	0.82	0.53	/
7	1.55	/	89.01	3.04	6.4	/

contained almost no MnO. Granular precipitates in the steel matrix were identified as primarily composed of SiO_2.

Fig. 4 shows the interfacial morphology between Si-Mn deoxidized steel and the CaO–SiO_2–Al_2O_3–MgO–MnO–FeO oxide system before and after heat treatment at 1273 K, 1373 K, and 1473 K for 10 h. The chemical compositions of the oxides adjacent to the interface and the precipitates formed in the steel matrix after heat treatment are presented in Tables 9-14. As shown in Fig. 4(a), (c), and (e), the interface between Si–Mn deoxidized steel and FeO-containing oxide also exhibits good bonding, with the oxide being homogeneous and no precipitates formed in the steel matrix. As shown in Fig. 4(b), (d), and (f), after heat treatment at 1273 K for 10 hours, a small amount of elongated precipitates was observed in the steel matrix near the interface of sample B0-10. These precipitates were identified as predominantly SiO_2,

Table 5. *Chemical composition (mass fraction / %) of each position in diffusion couple A1-0*

position	MgO	Al_2O_3	SiO_2	CaO	MnO	FeO
1	5.19	11.31	67.55	11.79	1.55	2.61
2	5.04	12.11	67.18	11.56	2	2.11
3	4.8	11.37	67.48	11.82	1.49	3.04
4	4.94	11.14	68.1	11.64	1.6	2.57

Table 6. *Chemical composition (mass fraction / %) of each position in diffusion couple A1-10*

position	MgO	Al_2O_3	SiO_2	CaO	MnO	FeO
1	10.55	7.56	61.87	16.21	2.53	1.28
2	10.06	7.84	64.41	14.15	2.01	1.52
3	2.39	12.61	71.44	10.78	0.55	2.23
4	2.76	10.17	75.46	9	0.62	1.99
5	2.68	12.22	70.77	10.91	0.87	2.55
6	2.92	10.75	72.3	10.14	1.07	2.83
7	12.15	/	73.21	1.46	13.18	/
8	/	/	85.92	/	14.08	/

with a mass fraction exceeding 99%. Additionally, the white particles at location 7 in the oxide were determined to be Fe particles. As the heat treatment temperature was increased to 1373 K, numerous dark particles precipitated in the steel matrix near the interface, primarily composed of SiO_2 and MnO. The size of these dark particles decreased with increasing distance from the interface. The oxide consists of both dark and gray phases. Compared to the pre-heat-treated sample B1-0, the dark phase near the interface exhibits an increased mass fraction of SiO_2, while the mass fractions of MgO, CaO, and MnO decrease. Furthermore, compared to the sample B0-10 heat-treated at 1273 K, more white particles have precipitated in the oxide. This indicates that when the heat treatment temperature increases from 1273 K to 1373 K with the same holding time of 10 h, a greater amount of Fe particles precipitates in the oxide. The gray phase in the oxide shows an increase in the mass fractions of MgO, CaO, and MnO, while the mass fractions of SiO_2 and Al_2O_3 decrease compared to the pre-heat-treated condition. When the heat treatment temperature is further raised to 1473 K, the dark particles precipitated in the oxide exhibit a larger size compared to those formed at 1373 K. The dark particles at locations 7 and 8 are primarily composed of SiO_2, with an average mass fraction of approximately 99%, along with about 1% MnO. In sample B2-10, the oxide near the interface is predominantly composed of the gray phase. Compared to the pre-heat-treated sample B2-0, the mass fraction of SiO_2 in the oxide decreases, while the mass fractions of Al_2O_3 and FeO increase. Additionally, a dark phase is observed in the oxide near the interface in B2-10, which is characterized by a high SiO_2 content with an average mass fraction

Table 7. *Chemical composition (mass fraction / %) of each position in diffusion couple A2-0*

position	MgO	Al_2O_3	SiO_2	CaO	MnO	FeO
1	5.13	11.77	66.33	12.23	2.72	1.82
2	5.08	12.41	65.84	12.19	2.5	1.98
3	5.31	12.36	66.69	11.98	2.22	1.43
4	5.26	12.16	65.73	12.48	2.38	2
5	5.56	12.43	65.7	12.39	2.28	1.64

Table 8. *Chemical composition (mass fraction / %) of each position in diffusion couple A2-10*

position	MgO	Al_2O_3	SiO_2	CaO	MnO	FeO
1	5.29	13.55	63.04	12.06	1.89	4.17
2	5.2	13.84	62.64	12.19	1.7	4.42
3	5.62	13.67	62.5	11.99	2.07	4.15
4	0.17	1.44	95.47	1.24	/	1.68
5	0.49	2.41	93.31	2.04	/	1.74
6	0.42	1.78	95.4	1.23	0.11	1.05
7	1.91	22.39	51.15	3.66	20.89	/
8	2.24	0.57	94.28	0.1	2.8	/

exceeding 95%. As shown in Tables 9-14, after isothermal heat treatment, the FeO content in the oxide near the interface increases compared to that before heat treatment in all samples.

3.2. The composition change at the interface between oxide and steel matrix after heat treatment

Figure 5 shows the compositional changes of oxides at the interface between the Si-Mn deoxidized steel matrix and oxide inclusions, as well as the variations of Si and Mn in the steel matrix, for the FeO-free diffusion couple samples after isothermal heat treatment at 1273, 1373, and 1473 K for 10 hours. As seen in Figures 5(a), (b), and (c), the mass fraction of FeO in the oxide tends to increase near the interface, with the most pronounced elevation observed in sample A1-10: at a distance of 3 μm from the interface, the FeO content reaches a maximum of 9.68%. In contrast, no significant compositional changes are observed in the oxide of sample A0-10. In sample A1-10, it can be observed that within approximately 18 μm from the interface, the mass fractions of SiO_2 and Al_2O_3 in the oxide decrease progressively toward the interface, declining from their maximum values of 71.82% and 13.43% to 66.64% and 9.29%, respectively. Meanwhile, the mass fraction of MnO stabilizes beyond about 25 μm from the interface. Within 25 μm of the interface, the MnO content decreases to below 2%. When the heat treatment temperature reached 1473 K and was held for 10 hours, as shown in Figure 5(c), it can be observed in sample A2-10 that the mass fractions of the various oxide components remained relatively

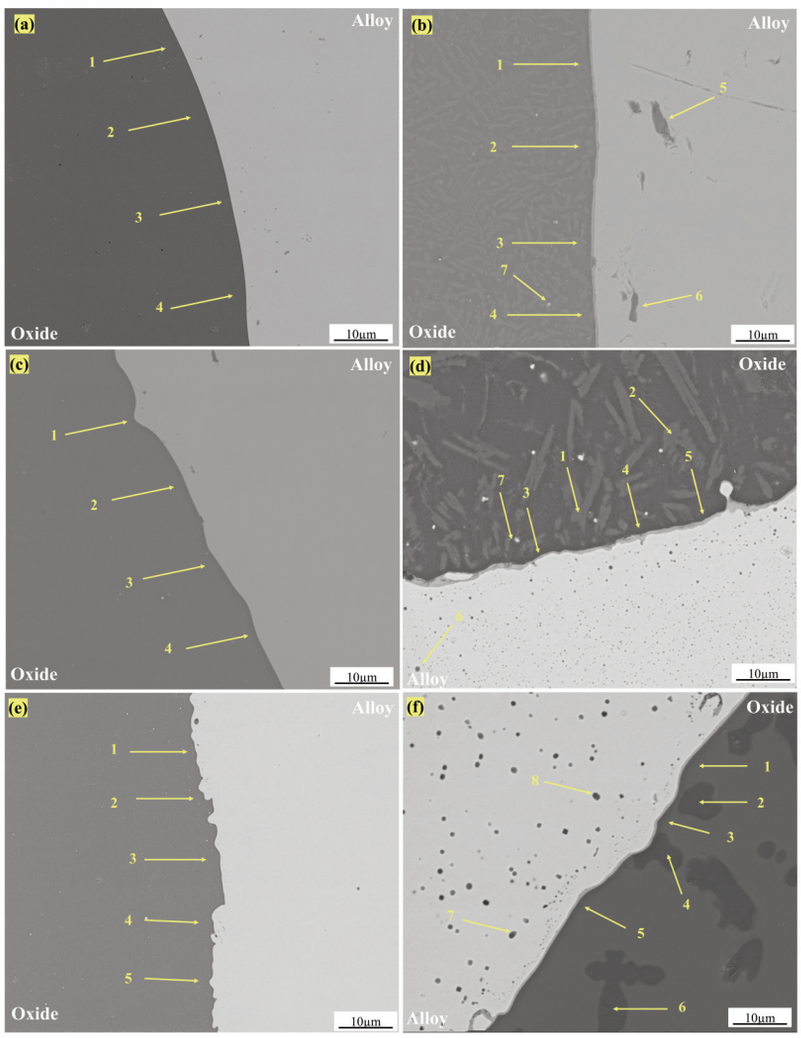

Figure 4. *The interface morphology between Si-Mn deoxidized steel and CaO-SiO_2-Al_2O_3-MgO-MnO-FeO oxide before heat treatment and after heat treatment at 1273 K, 1373 K, 1473 K for 10 h: (a) B0-0; (b) B0-10; (c) B1-0; (d) B1-10; (e) B2-0; (f) B2-10*

Table 9. *Chemical composition (mass fraction / %) of each position in diffusion couple B0-0*

position	MgO	Al_2O_3	SiO_2	CaO	MnO	FeO
1	4.84	11.21	67.03	13.06	2.61	1.24
2	5.13	11.45	67.83	12.02	2.42	1.15
3	4.92	11.59	66.98	12.83	2.19	1.49
4	4.58	11.79	67.04	12.84	2.58	1.17

Table 10. *Chemical composition (mass fraction / %) of each position in diffusion couple B0-10*

position	MgO	Al_2O_3	SiO_2	CaO	MnO	FeO
1	9.09	10.72	58.94	14.17	2.93	4.15
2	9.21	10.47	58.1	12.65	3.73	5.85
3	1.11	15.44	67.5	10.96	1.66	3.34
4	10.11	8.54	55.75	13.51	4.47	7.62
5	/	0.17	99.78	/	0.05	/
6	/	/	99.72	/	0.28	/

Table 11. *Chemical composition (mass fraction / %) of each position in diffusion couple B1-0*

position	MgO	Al_2O_3	SiO_2	CaO	MnO	FeO
1	4.85	11.28	65.89	12.9	1.68	3.41
2	5.05	10.72	63.89	13.74	1.87	4.73
3	4.62	11	61.95	12.93	2.03	7.46
4	4.85	11.21	65.14	13.29	1.89	3.62

Table 12. *Chemical composition (mass fraction / %) of each position in diffusion couple B1-10*

position	MgO	Al_2O_3	SiO_2	CaO	MnO	FeO
1	12.11	6.71	58.46	13.53	4.68	4.51
2	13.44	5.78	58.73	16.05	3.22	2.78
3	2.78	12.1	68.48	10.25	1.44	4.95
4	1.08	12.18	73.4	8.57	0.56	4.2
5	0.5	13.91	72	8.77	0.51	4.31
6	8.03	5.68	62.23	4.63	19.42	/

Table 13. *Chemical composition (mass fraction / %) of each position in diffusion couple B2-0*

position	MgO	Al_2O_3	SiO_2	CaO	MnO	FeO
1	5.2	11.69	66.31	12.02	1.62	3.17
2	5.19	11.94	66.55	11.84	1.66	2.81
3	5.18	11.81	65.57	11.92	1.79	3.73
4	4.62	11.82	66.88	11.6	1.76	3.32
5	4.83	12.31	65.86	11.79	1.74	3.46

Table 14. *Chemical composition (mass fraction / %) of each position in diffusion couple B2-10*

position	MgO	Al_2O_3	SiO_2	CaO	MnO	FeO
1	4.86	13.54	61.05	12.94	1.79	5.82
2	0.23	1.37	95.46	1.26	/	1.68
3	4.61	13.14	62.02	13.01	1.79	5.42
4	/	1.43	96.26	0.85	0.16	1.3
5	4.72	13.35	61.96	12.85	2.04	5.08
6	0.19	1.61	96.1	1.06	0.23	0.81
7	/	/	98.73	0.14	1.12	/
8	/	/	99.31	/	0.69	/

stable within approximately 30 μm from the interface and beyond 60 μm. In the region between about 30 μm and 60 μm from the interface, the mass fraction of FeO exhibited an overall increasing trend. Closer to the interface, the mass fractions of MnO, CaO, and

from Figure 6(a), in samples that underwent oxide premelting but no subsequent heat treatment soaking,

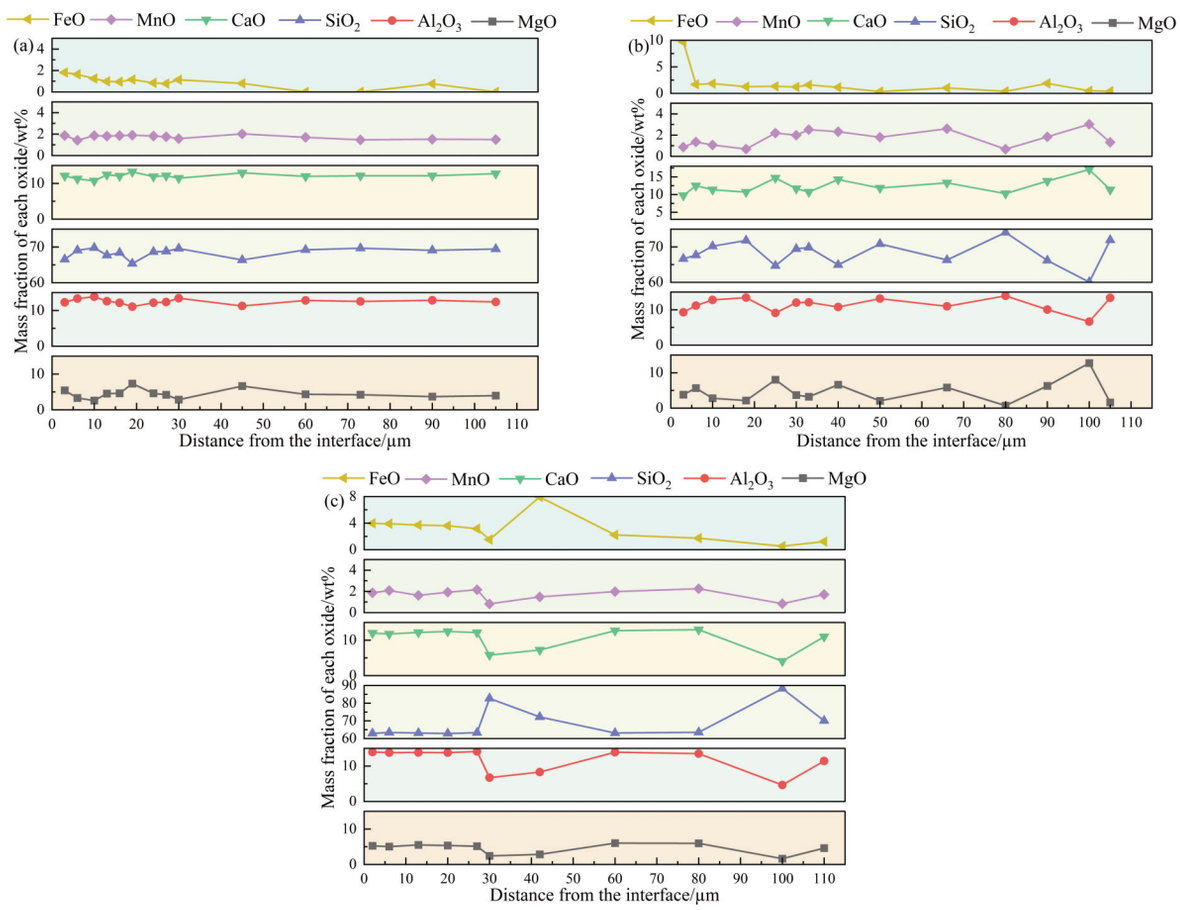

Figure 5. *The composition change of oxides near the interface (a) A0-10; (b) A1-10; (c) A2-10*

Al_2O_3 decreased, reaching minimum values of 0.83%, 5.80%, and 6.73%, respectively, while the mass fraction of SiO_2 increased, attaining a maximum value of 82.71%.

Figure 6 (a) and (b) show the variation curves of silicon and manganese contents in the steel matrix near the interface between the Si-Mn deoxidized steel and the CaO-SiO_2-Al_2O_3-MgO-MnO oxide. As seen the mass fraction of silicon in the steel matrix shows an increasing trend near the interface. After samples A0-0 and A1-0 were subjected to heat treatment at 1273 K for 10 h and 1373 K for 10 h, respectively, the variation trend of the silicon mass fraction in the steel matrix did not change significantly. However, the stabilized silicon content away from the interface was

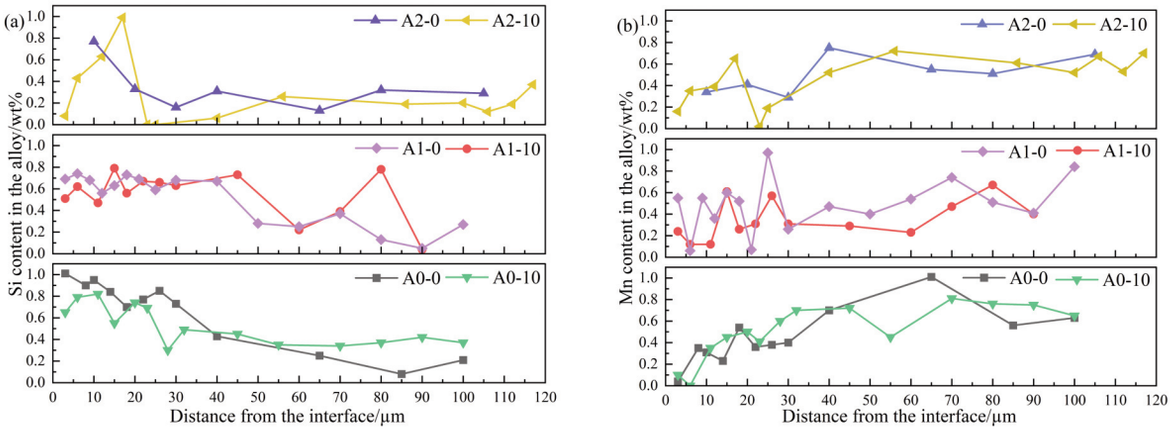

Figure 6. *Variations of Mn and Si contents in the steel matrix near the interface: (a) Change in Si content in the steel matrix of the diffusion couple without FeO before and after heat treatment; (b) Change in Mn content in the steel matrix of the diffusion couple without FeO before and after heat treatment*

slightly higher compared to that before the heat treatment. Upon heat treatment at 1473 K for 10 h, the silicon content in the steel matrix of sample A2-0 did not increase immediately. Instead, a concentration peak emerged at approximately 17 μm from the interface, reaching a maximum value of 0.99%, before decreasing to around 0.2% and subsequently stabilizing. The variation in manganese content in the steel matrix near the interface is shown in Figure 6(b). After the diffusion couple sample A0-0 was heat-treated at 1273 K for 10 hours to obtain sample A0-10, a comparison of the manganese mass fraction curves indicates no significant difference in the manganese content of the steel matrix before and after heat treatment. Both curves exhibit similar trends: the manganese mass fraction decreases progressively near the interface and stabilizes beyond approximately 40 μm from the interface. When the heat treatment temperature reaches 1373 K, the manganese content in the steel matrix within 80 μm of the interface decreases slightly compared with that before heat treatment, and is lower than the initial manganese content. In sample A2-0, the manganese content is lower than the initial value within a region extending approximately 40 μm from the interface. After heat treatment at 1473 K for 10 h, the manganese content in sample A2-10 exhibits an overall decreasing trend within about 56 μm from the interface. Compared to the condition before heat treatment, the affected distance over which the manganese content decreases is extended. The mass fraction of manganese declines within 17 μm of the interface, reaching a minimum value of approximately 0.16% at a distance of 3 μm.

Figure 7 (a), (b), and (c) show the compositional variations of different oxides at the interface between the Si-Mn deoxidized steel matrix and the oxide in diffusion couple samples containing 3% FeO after 10 hours of heat treatment at 1273 K, 1373 K, and 1473 K, respectively. As shown in the figure, after heat treatment at 1273 K and 1373 K for 10 hours, the FeO content in the oxide of the samples increases significantly near the interface. In samples B0-10 and B1-10, the mass fraction of FeO stabilizes near the initial FeO level beyond approximately 5 μm from the interface. Within about 5 μm of the interface, the FeO mass fraction rises, reaching a maximum value of 17.55% at approximately 3 μm from the interface in sample B0-10, and 10.02% at about 2 μm from the interface in sample B1-10. At a heat treatment temperature of 1473 K, the mass fraction of FeO was consistently higher than the initial FeO content and continued to increase within approximately 4 μm of the interface. In sample B0-10, the mass fractions of MnO, CaO, and MgO remained stable beyond about 5 μm from the interface, decreased within 5 μm, and reached their minimum values near the interface at approximately 3 μm, measuring 0.98%, 8.48%, and 1%, respectively. The mass fraction of SiO_2 stabilized beyond around 10 μm from the interface, decreased continuously within 10 μm, and reached a minimum of about 59.44% at approximately 3 μm from the interface. In contrast, the mass fraction of Al_2O_3 in B0-10 remained relatively stable throughout. The mass fractions of MnO, CaO and MgO in B1-10 vary similarly near the interface, but the decreasing range is prolonged: it tends to be stable outside about 9μm near the interface, decreases within 9μm, and reaches the lowest value at about 2 μm near the interface, which is 0.48%, 7.48% and 0.52% respectively. The mass fraction of SiO_2 increases at about 9μm near the interface, reaching more than 70% as a whole, and the mass fraction of Al_2O_3 is relatively stable. As shown in Fig. 7(c), the composition of each oxide in sample B2-10 remains relatively stable with decreasing distance to the interface, indicating a homogeneous

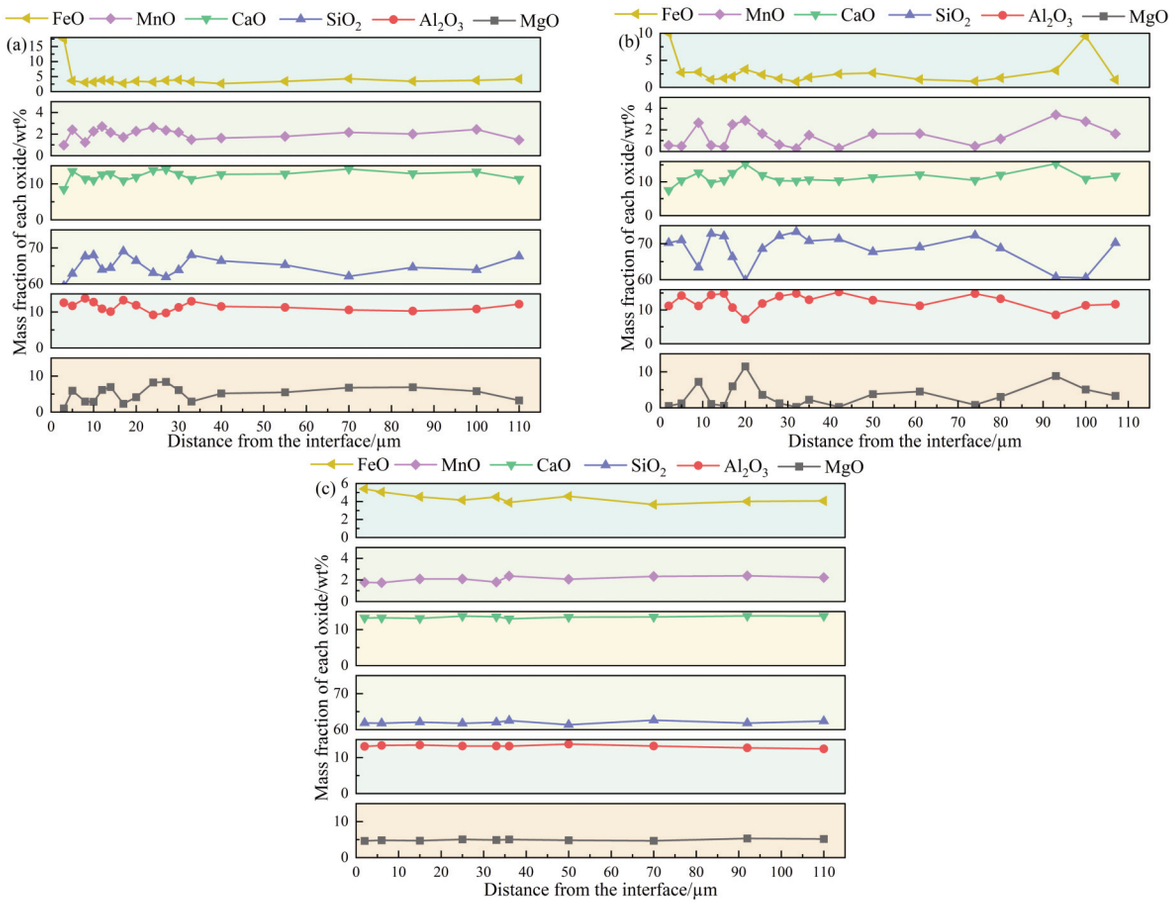

Figure 7. *The composition change of oxides near the interface (a) B0-10; (b) B1-10; (c) B2-10*

distribution of oxide components after heat treatment at 1473 K for 10 hours. The overall mass fractions of MnO, CaO, and Al_2O_3 are higher than their initial contents, while those of SiO_2 and MgO are lower.

Figure 8(a) and (b) illustrate the variations in silicon and manganese contents within the steel matrix near the interface between Si-Mn deoxidized steel and the CaO–SiO_2–Al_2O_3–MgO–MnO–FeO oxide. As observed in Fig. 8(a), prior to the heat treatment soaking process but after the oxide premelting experiment, the overall mass fraction of silicon in the steel matrix was higher than its initial content. After sample B0-0 underwent the heat treatment experiment at 1273 K for 10 hours, the overall mass fraction of silicon in the steel matrix decreased compared to that before the heat treatment. Beyond approximately 60 μm from the interface, the silicon content stabilized near its initial level. Within about 60 μm of the interface, the silicon mass fraction increased continuously, reaching a maximum value of approximately 0.57% at a distance of 2 μm. In samples B1-10 and B2-10, a “peak” in the silicon mass fraction was observed in the steel matrix near the interface. In samples B1-10 and B2-10, the silicon mass fraction in the steel matrix will appear a ‘ peak ‘ at the boundary. It can be seen from the diagram that silicon will not rise immediately near the interface, but reached its maximum at distance of 20 μm and 5 μm away from the interface, respectively. The maximum silicon mass fractions in the steel matrix of B1-10 and B2-10 reached 0.64% and 1.94%, respectively.

As shown in Figure 8(b), the mass fraction of manganese in the steel matrix decreased near the interface in all diffusion couple samples after heat treatment. In sample B0-10, the manganese content stabilized beyond approximately 22 μm from the interface. Within about 22 μm of the interface, the manganese mass fraction decreased continuously, dropping to approximately 0% at a distance of around 8 μm from the interface. In B1-10, the mass fraction of manganese is lower than the initial manganese content in the ranges of about 16μm and 25 ~ 60 μm near the interface. The relatively dispersed data points of sample B1-10 indicate that the Si and Mn contents in the steel matrix at the interface after heat treatment

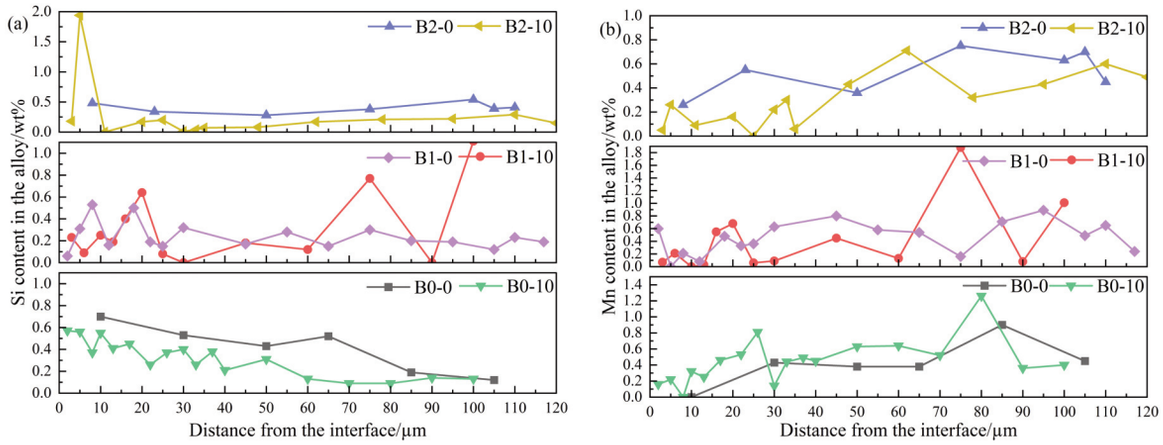

Figure 8. *Variations in Mn and Si contents in the steel matrix near the interface: (a) Change of Si content in the steel matrix of the FeO-containing diffusion couple before and after heat treatment; (b) Change of Mn content in the steel matrix of the FeO-containing diffusion couple before and after heat treatment*

at 1373 K for 10 h are not uniform. In B2-10, the mass fraction of manganese in the steel matrix tends to be stable beyond about 48 μm from the interface, and the overall mass fraction of manganese decreases within about 48 μm from the interface, remaining lower than the initial manganese content.

4. Discussion

4.1. The relationship between the particle precipitation zone and the Mn element consumption zone at the interface

Figure 9 shows the width of the precipitate zone in the steel matrix at the interface after heat treatment. To better characterize the precipitate zone width under different heat treatment conditions and across various diffusion couples, observations were conducted using multiple fields of view in scanning electron microscopy. The samples A0-10 and B0-10 were observed at a magnification of 4000x using scanning electron microscopy, as shown in Fig. 9(a) and (d). The width of the precipitate zone in A0-10 is approximately 8 μm. Here, the region near the interface in the steel matrix where oxide particles have precipitated is defined as the particle precipitation zone (PPZ). The PPZ width in B0-10 is measured to be 18 μm. Samples A1-10, B1-10, A2-10, and B2-10 were observed at a magnification of 1000x using scanning electron microscopy. As shown in Fig. 9(b) and (e), when the heat treatment temperature was increased to 1373 K, the width of the PPZ in both samples A1-10 and B1-10 extended beyond 100 μm. Additionally,numerous white Fe particles were observed to precipitate at the interface in sample B1-10. At a heat treatment temperature of 1473 K, the PPZ widths in samples A2-10 and B2-10 were 35 μm and 70 μm, respectively. Comparing diffusion couple samples with different compositions under the same heat treatment conditions shows that, when the conditions were identical, the samples with an initial oxide composition containing 3% FeO exhibited a larger PPZ width. Meanwhile, diffusion couple samples with an initial oxide composition containing no FeO also developed a certain PPZ width after heat treatment at different temperatures. This can be attributed to the formation of a certain amount of FeO at the interface during the preparation of the diffusion couples—specifically, in the oxide pre-melting experiment conducted prior to the heat treatment. For a given diffusion couple, the width of the precipitated particle zone (PPZ) varied under different heat treatment conditions. However, regardless of whether the initial oxide composition of the diffusion couple contained FeO or not, the PPZ width in the steel substrate reached its maximum after heat treatment at 1373 K for 10 hours. For both types of diffusion couples, the manganese (Mn) content in the steel substrate near the interface decreased to varying extents under different heat treatment conditions. This region of reduced Mn concentration in the steel substrate is defined as the manganese-depleted zone (MDZ). Figure 10 illustrates the variations in the widths of the particle precipitation zone (PPZ) and the manganese-depleted zone (MDZ) in the steel substrate near the interface between Si-Mn deoxidized steel and the two oxide systems $CaO\text{-}SiO_2\text{-}Al_2O_3\text{-}MgO\text{-}MnO$ and $CaO\text{-}SiO_2\text{-}Al_2O_3\text{-}MgO\text{-}MnO\text{-}FeO$ after 10 hours of heat treatment at 1273 K, 1373 K, and 1473 K. The results indicate an approximately linear correlation between the MDZ and PPZ widths after heat treatment. Moreover, regardless of whether the initial oxide composition of the diffusion couple contained FeO, both the MDZ and PPZ widths in the steel substrate reached their maximum values following the heat treatment at 1373 K for 10 hours. At heat treatment temperatures of 1273 K and 1473 K,

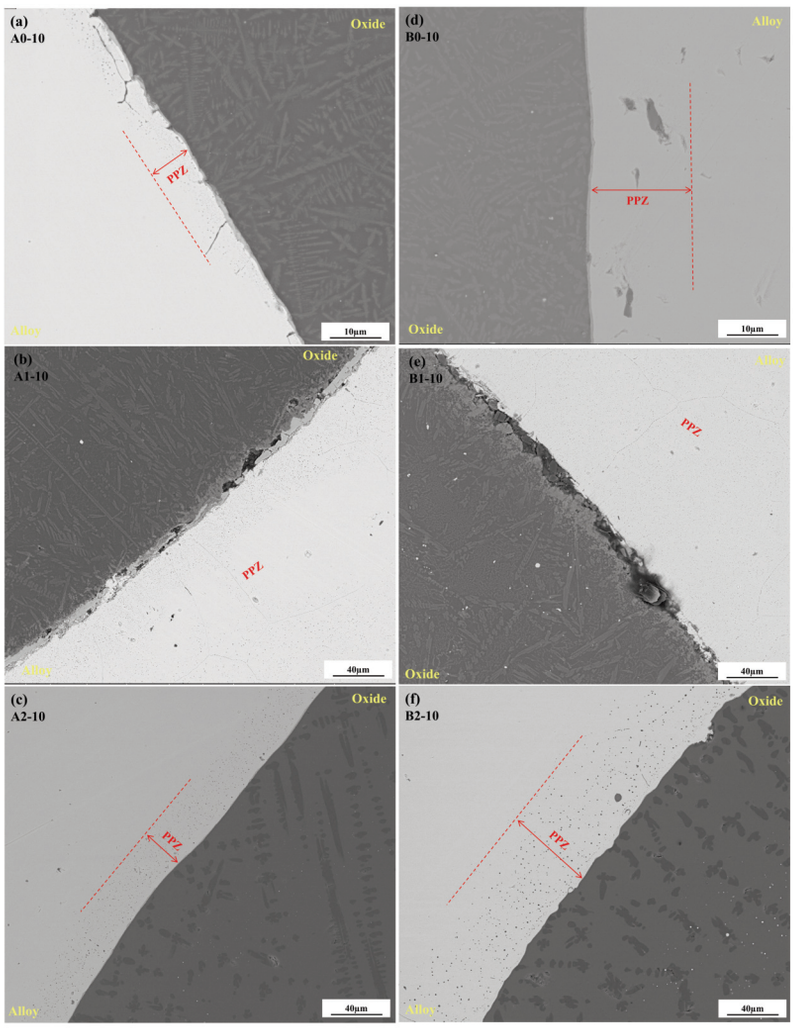

Figure 9. *The precipitation of particles at the interface between Si-Mn deoxidized steel and CaO-SiO_2-Al_2O_3-MgO-MnO and CaO-SiO_2-Al_2O_3-MgO-MnO-FeO oxides after heat treatment at 1273 K, 1373 K and 1473 K for 10 h (a) A0-10; (b) A1-10; (c) A2-10; (d) B0-10; (e) B1-10; (f) B2-10*

the widths of both the manganese-depleted zone (MDZ) and the particle precipitation zone (PPZ) in the steel substrate were larger in diffusion couples with an initial FeO content of 3% than in those without FeO. In the present study, the maximum MDZ width—that is, the maximum extent of manganese depletion was achieved after heat treatment at 1373 K for 10 hours. This pronounced manganese depletion facilitates the nucleation of intragranular ferrite (IGF). Therefore, the heat treatment temperature should be set at approximately 1373 K.

4.2. The mechanism of solid-state reaction between Si-Mn deoxidized steel and complex oxide

In this study, after heat treatment, a significant number of oxide particles formed at the interface between Si–Mn deoxidized steel and two types of oxide systems—CaO–SiO_2–Al_2O_3–MgO–MnO and CaO–SiO_2–Al_2O_3–MgO–MnO–FeO. This interfacial reaction led to noticeable changes in the Si and Mn contents in the steel matrix, as well as alterations in the oxide composition. According to previous studies [12] these phenomena can be attributed to disruption of equilibrium at the steel–oxide interface and the occurrence of a solid-state reaction when the heat treatment temperature is below 1873 K.

When the initial oxide composition contains no FeO, silicon in the steel matrix near the interface with the oxides reacts with MnO in the oxides [14] , as represented by Equation (1).

$$[\mathrm{Si}] + 2\mathrm{MnO} = 2[\mathrm{Mn}] + \mathrm{SiO_2} \quad (1)$$

This leads to an increase in the SiO_2 content within

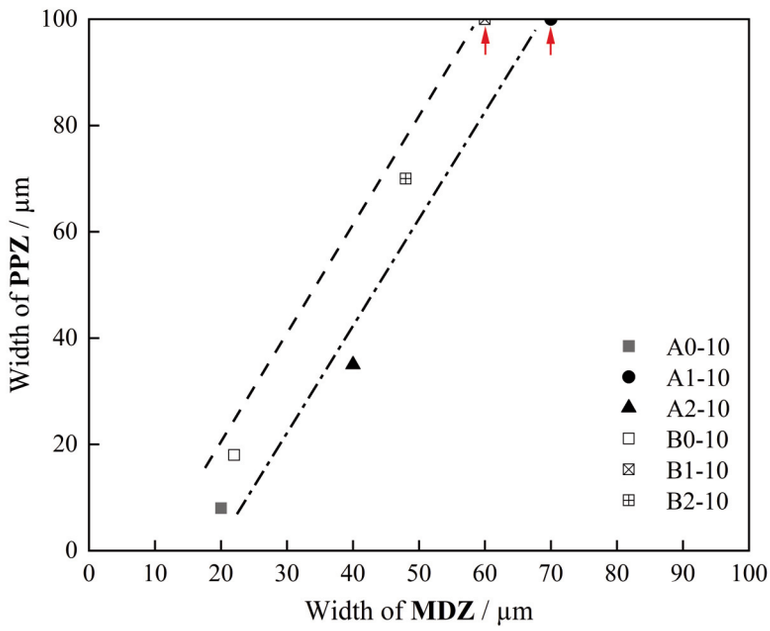

Figure 10. *The consumption zone of Mn element in Si–Mn deoxidized steel and the width of particle precipitation zone in CaO-SiO_2-Al_2O_3-MgO-MnO and CaO-SiO_2-Al_2O_3-MgO-MnO-FeO oxides after heat treatment at 1273 K, 1373 K and 1473 K for 10 h*

the oxides near the interface. However, after the fabrication of the diffusion couple—i.e., the pre-melting experiment of the oxide—oxygen released from the decomposition of CaO, MgO, and Al_2O_3 in the oxides reacts with iron in the steel matrix to form iron oxide (FeO_x). As a result, a small amount of FeO forms in the oxide phase adjacent to the interface.

When the initial oxide composition contains FeO, the oxygen activity (a_O) and FeO activity (a_{FeO}) in the equilibrium system between Si-Mn deoxidized steel and oxide inclusions at a given temperature and oxygen partial pressure were calculated using FactSage 8.0 with the FToxide and FTmisc databases, based on relevant thermodynamic data. The calculated oxygen activity (a_O) in the Si-Mn deoxidized steel at 1873 K is 1.73×10^{-6}, and the activity of FeO (a_{FeO}) in the oxide is 2.15×10^{-2}. Due to the lack of thermodynamic data for this system at lower temperatures, the fundamental thermodynamic parameters obtained at 1873 K were applied to estimate the behavior at reduced temperatures. The resulting trends of a_O and a_{FeO} as functions of temperature are shown in Figure 11.

As shown in Figure 11, a decrease in temperature leads to a sharp reduction in the equilibrium oxygen activity (a_O) in the steel matrix. When the temperature drops from 1873 K to 1473 K, 1373 K, and 1273 K, the corresponding a_O values decrease to 1.06×10^{-8}, 9.12×10^{-9}, and 1.56×10^{-9}, respectively. The decline in oxygen activity causes the excess oxygen in the steel to react with elements such as manganese, silicon, and iron, forming additional oxides. As a result, the mass fractions of SiO_2, MnO, and FeO near the interface increase. As can also be seen from Figure 11, when the temperature decreases from 1873 K to 1473 K, the activity of FeO (a_{FeO}) in the oxide decreases from 2.15×10^{-2} to 7.85×10^{-3}. The decrease in FeO activity leads to the decomposition of FeO into Fe and [O], as shown in Equation (2).

$$FeO = Fe + [O] \tag{2}$$

Subsequently, Fe particles form within the oxides. As the heat treatment proceeds, the oxygen [O] generated from the decomposition of FeO diffuses to the steel matrix interface, where it reacts with Si and Mn to form silicate and manganese oxide particles, as shown in Equations (3) and (4).

$$Si + 2[O] = SiO_2 \tag{3}$$

$$Mn + [O] = MnO \tag{4}$$

The entire reaction process [29, 30] can be represented by the following equation:

$$3FeO+Mn+Si=MnO\cdot SiO_2+3Fe \tag{5}$$

This leads to a decrease in the Si and Mn contents in the steel matrix near the interface, resulting in the formation of a Mn-depleted zone [29]. This observation is consistent with the decrease in the mass fractions of Si and Mn near the interface after heat

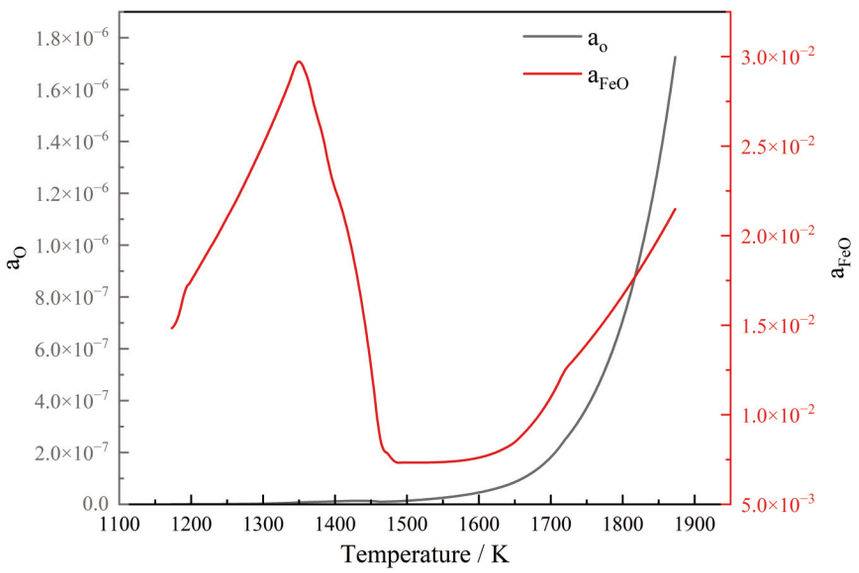

Figure 11. *The variation of oxygen activity in steel and FeO activity in CaO-SiO_2-Al_2O_3-MgO-MnO-FeO with temperature during the equilibrium of 3% FeO diffusion couple*

treatment, as shown in Figures 8(a) and 9(b) compared to the initial state. At temperatures of 1273 K and 1373 K, the activity of FeO (a_{FeO}) in the oxide was measured as 2.28 × 10^{-2} and 2.70 × 10^{-2}, respectively, indicating an increase compared to that at 1873 K. Nevertheless, a certain amount of particulate precipitates was observed in the steel matrix, with the most pronounced precipitation occurring at 1373 K. This phenomenon can be attributed to the participation of SiO_2 from the oxide in the precipitate formation process, which consumes SiO_2 near the interface [28]. In this study, due to the high SiO_2 content in the designed diffusion couple, the particulate precipitates formed in the steel matrix were predominantly composed of SiO_2 and exhibited relatively low MnO content. The reaction mechanism at the interface between the steel matrix and the oxide in the diffusion couple with no initial FeO is illustrated in Figure 12. For the diffusion couple containing 3% initial FeO in the oxide phase, the corresponding interfacial reaction mechanism is shown in the FeO-containing part of Figure 12.

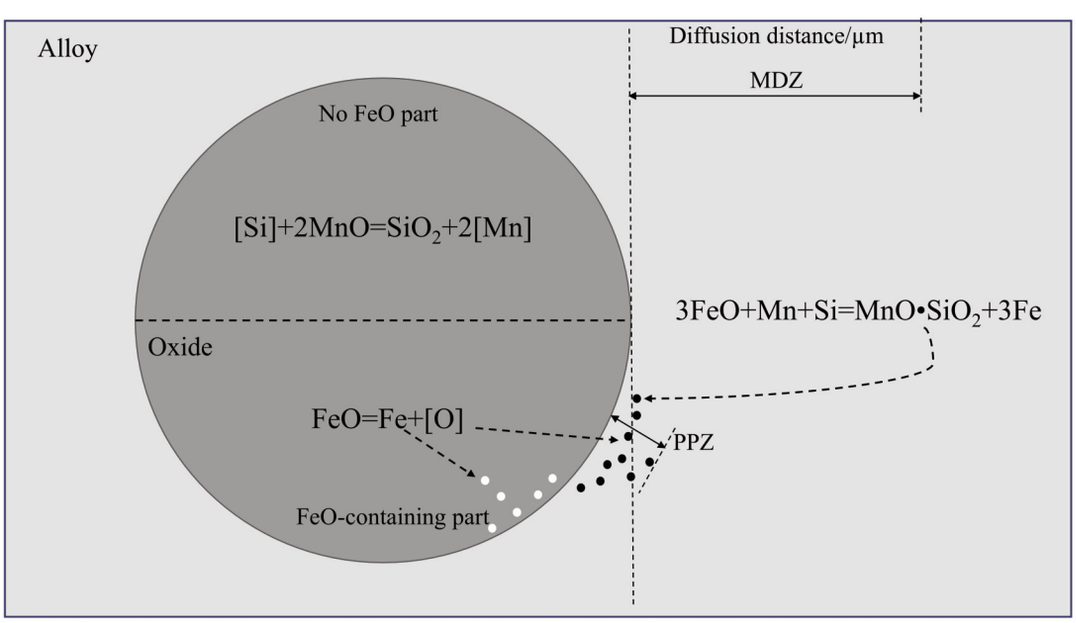

Figure 12. *The reaction mechanism between the matrix and the oxide interface of the sample steel without FeO diffusion couple in the initial oxide composition*

5. Conclusion

In the present study, the evolution of interfacial morphology and composition in Si-Mn deoxidized steel in contact with CaO-SiO_2-Al_2O_3-MgO-MnO and CaO-SiO_2-Al_2O_3-MgO-MnO-FeO oxide systems were investigated after isothermal holding at 1273, 1373, and 1473 K for 10 hours. The following results were obtained.

(1) After isothermal holding at 1273, 1373, and 1473 K for 10 hours, precipitates were observed in the steel matrix for both the quinary (CaO-SiO_2-Al_2O_3-MgO-MnO) and senary (CaO-SiO_2-Al_2O_3-MgO-MnO-FeO) oxide systems. The precipitates consisted predominantly of SiO_2 with minor amounts of MnO. A dark phase with high SiO_2 content was also identified in the oxide region near the interface. Notably, in the diffusion couple with FeO-containing initial oxides, a greater number of Fe particles precipitated in the oxides adjacent to the interface.

(2) After the pre-melting experiment with the quinary oxide system CaO-SiO_2-Al_2O_3-MgO-MnO, a certain amount of FeO precipitated in the oxide region near the interface with the steel matrix. Following heat treatment, all diffusion couple samples exhibited fluctuations in the composition of the oxide near the interface to varying degrees. These compositional changes were most pronounced at 1373 K and most stable at 1473 K.

(3) Regardless of whether the initial oxide composition in the diffusion couple samples contained FeO, the widths of the MDZ and PPZ after heat treatment exhibited an approximately linear correlation. Under the condition of isothermal holding at 1373 K for 10 hours, both the MDZ and PPZ widths in the steel matrix reached their maximum values. Moreover, under identical heat treatment conditions, the samples with an initial oxide composition containing 3% FeO showed larger MDZ and PPZ widths than those without FeO.

Acknowledgments

We would like to express our sincere gratitude to Dr. Qi Xu and Dr. Shannan Li for his invaluable suggestions and guidance in the revision of this thesis. Special thanks to the staff at the Room 721, Steel Building, Wuhan University of Science and Technology for their technical assistance during the experimental phase.

Funding

This work was financially supported by the National Natural Science Foundation of China (52404350), Research Project of Hubei Provincial Department of Science and Technology (2024CSA083), Research Project of Hubei Provincial Department of Education (D20231101).

Conflict of Interest

The authors declare that they have no conflict of interest.

Data Availability Statement

The data generated and analyzed during the current study are not publicly available due to proprietary information but are available from the corresponding author on reasonable request.

Author contribution statement

Xinlong Nie conceived and designed the study, analyzed the data, and wrote the manuscript; Xinlong Nie collected the data and contributed to the interpretation of results; Shannan Li and Qi Xu provided valuable suggestions and revised the manuscript for intellectual content; Jianli Li supervised the project and obtained funding.

Authors ORCID

Xinlong Nie (0009-0001-8576-4354), Shannan Li (0009-0005-7553-5549), Qi Xu (0009-0005-6539-659X), Jianli Lia (0000-0002-9952-1126)

References

[1] A.V. Amezhnov, I.G. Rodionova, D.V. Kuznetsov, A.A. Komissarov, E.P. Sidorova, Effect of heat treatment on corrosion activity of nonmetallic inclusions and steel corrosion resistance in aqueous media, Metallurgist, 62 (11) (2019) 1232–1239. https://doi.org/10.1007/s11015-019-00779-x

[2] W. Choi, H. Matsuura, F. Tsukihashi, Changing behavior of non–metallic inclusions in solid iron deoxidized by Al–Ti addition during heating at 1473 K, ISIJ International, 51 (12) (2011) 1951–1956. https://doi.org/10.2355/isijinternational.51.1951

[3] L. Cheng, W. Li, L. Zhang, Y. Ren, Effect of sulfur content on evolution of nonmetallic inclusions in low sulfur Al–killed steels during heat treatment, Steel Research International, 93 (5) (2022) 2100526. https://doi.org/10.1002/srin.202100526

[4] H. Shibata, K. Kimura, T. Tanaka, S.Y. Kitamura, Mechanism of change in chemical composition of oxide inclusions in Fe–Cr alloys deoxidized with Mn and Si by heat treatment at 1473 K, ISIJ International, 51(12) (2011) 1944–1950. https://doi.org/10.2355/isijinternational.51.1944

[5] G. Song, Z. Deng, M. Zhu, Effect of ladle washing operation on non–metallic inclusions in tire cord steel: laboratory simulation, Metallurgical and Materials Transactions B, 55 (4) (2024) 2805–2816. https://doi.org/10.1007/s11663-024-03143-w

[6] X. Wang, Z. Deng, M. Zhu, Evolution of nonmetallic

inclusions in high Mn–high Al steel during heat treatment, Ironmaking & Steelmaking, 52 (2) (2025) 260–271. https://doi.org/10.1177/03019233241273487

[7] Y. Meng, J. Li, K. Wang, H. Zhu, Effect of the bloom–heating process on the inclusion size of Si–killed spring steel wire rod, Metallurgical and Materials Transactions B, 53 (4) (2022) 2647–2656. https://doi.org/10.1007/s11663-022-02557-8

[8] H. Ono, K. Nakajima, T. Ibuta, T. Usui, Equilibrium relationship between the oxide compounds in MgO–Al_2O_3–Ti_2O_3 and molten iron at 1873 K, ISIJ International, 50 (12) (2010) 1955–1958. https://doi.org/10.2355/isijinternational.50.1955

[9] J.S. Park, J.H. Park, Effect of slag composition on the concentration of Al_2O_3 in the inclusions in Si–Mn–killed steel, Metallurgical and Materials Transactions B, 45 (3) (2014) 953–960. https://doi.org/10.1007/s11663-013-9998-2

[10] K. Wang, M. Jiang, X. Wang, Y. Wang, H. Zhao, Z. Cao, Formation mechanism of SiO_2–type inclusions in Si–Mn–killed steel wires containing limited aluminum content, Metallurgical and Materials Transactions B, 46 (5) (2015) 2198–2207. https://doi.org/10.1007/s11663-015-0411-1

[11] H.S. Kim, H.G. Lee, K.S. Oh, MnS precipitation in association with manganese silicate inclusions in Si/Mn deoxidized steel, Metallurgical and Materials Transactions A, 32 (6) (2001) 1519–1525. https://doi.org/10.1007/s11661-001-0239-y

[12] K.H. Kim, S.J. Kim, H. Shibata, S.Y. Kitamura, Reaction between MnO–SiO_2–FeO oxide and Fe–Mn–Si solid alloy during heat treatment, ISIJ International, 54 (10) (2014) 2144–2153. https://doi.org/10.2355/isijinternational.54.2144

[13] C. Lee, S. Nambu, J. Inoue, T. Koseki, Ferrite formation behaviors from B1 compounds in steels, ISIJ International, 51 (12) (2011) 2036–2041. https://doi.org/10.2355/isijinternational.51.2036

[14] C. Liu, H. Ni, S. Yang, J. Li, F. Ye, Interfacial reaction mechanism between multi–component oxides and solid alloys deoxidised by Mn and Si during heat treatment, Ironmaking & Steelmaking, 45 (3) (2018) 195–203. https://doi.org/10.1080/03019233.2016.1271968

[15] J.H. Park, D.S. Kim, Effect of CaO–Al_2O_3–MgO slags on the formation of MgO–Al_2O_3 inclusions in ferritic stainless steel, Metallurgical and Materials Transactions B, 36 (4) (2005) 495–502. https://doi.org/10.1007/s11663-005-0041-0

[16] Y. Wang, L. Zhang, Y. Ren, H. Duan, Q. Zhou, Solid reactions between CaO–Al_2O_3 and Si–Ti–containing steel at 1273 K, Journal of Materials Research and Technology, 18 (2022) 159–170. https://doi.org/10.1016/j.jmrt.2022.02.084

[17] W. Yang, C. Guo, L. Zhang, H. Ling, C. Li, Evolution of oxide inclusions in Si-Mn killed steels during hot–rolling process, Metallurgical and Materials Transactions B, 48 (5) (2017) 2717–2730. https://doi.org/10.1007/s11663-017-1025-6

[18] Z. Duan, C. Man, H. Cui, Z. Cui, X. Wang, Formation mechanism of MnS inclusion during heat treatments and its influence on the pitting behavior of 316L stainless steel fabricated by laser powder bed fusion, Corrosion Communications, 7 (2022) 12–22. https://doi.org/10.1016/j.corcom.2022.04.002

[19] F. Song, C. Yin, F. Hu, K. Wu, Effects of Mn–depleted zone formation on acicular ferrite transformation in weld metals under high heat input welding, Materials, 15 (23) (2022) 8477. https://doi.org/10.3390/ma15238477

[20] Y. Kang, K. Han, J.H. Park, C. Lee, Mn–depleted zone formation in rapidly cooled high–strength low–alloy steel welds, Metallurgical and Materials Transactions A, 45 (11) (2014) 4753–4757. https://doi.org/10.1007/s11661-014-2470-3

[21] S.J. Kim, H. Tago, K.H. Kim, S.Y. Kitamura, H. Shibata, Diffusion behavior of Mn and Si between liquid oxide inclusions and solid iron-based alloy at 1473 K, Metallurgical and Materials Transactions B, 49 (3) (2018) 977–987. https://doi.org/10.1007/s11663-018-1233-8

[22] C.S. Liu, K.H. Kim, S.J. Kim, J.S. Li, S.Y. Kitamura, Reaction between MnO–SiO_2–FeO solid oxide and solid steel deoxidized by Si and Mn during heat treatment at 1473 K (1200 °C), Metallurgical and Materials Transactions B, 46 (4) (2015) 1875–1884. https://doi.org/10.1007/s11663-015-0356-4

[23] C.S. Liu, S.F. Yang, K.H. Kim, J.S. Li, H. Shibata, S.Y. Kitamura, Influence of FeO and sulfur on solid state reaction between MnO−SiO_2−FeO oxides and an Fe−Mn−Si solid alloy during heat treatment at 1473 K, International Journal of Minerals, Metallurgy, and Materials, 22 (8) (2015) 811–819. https://doi.org/10.1007/s12613-015-1138-3

[24] J.S. Park, J.H. Park, Effect of slag composition on the concentration of Al_2O_3 in the inclusions in Si–Mn–killed steel, Metallurgical and Materials Transactions B, 45 (3) (2014) 953–960. https://doi.org/10.1007/s11663-013-9998-2

[25] K.H. Kim, H. Shibata, S.Y. Kitamura, Influence of sulfur on the reaction between MnO–SiO_2–FeO oxide and Fe–Mn–Si solid alloy by heat treatment, ISIJ International, 54 (12) (2014) 2678–2686. https://doi.org/10.2355/isijinternational.54.2678

[26] X.L. Zhang, S.F. Yang, C.S. Liu, J.S. Li, Q. Liu, G. Liu, Interfacial reaction between oxide inclusion and steel matrix deoxidized by Si and Mn at 1473 K, Journal of Iron and Steel Research International, 25 (1) (2018) 1–8. https://doi.org/10.1007/s42243-017-0005-z

[27] W. Wang, H. Zhu, J. Zhou, M. Song, L. Wang, Interaction between oxide inclusions and low-density steel during heat treatment, Metallurgical and Materials Transactions B, 53 (5) (2022) 2991–3002. https://doi.org/10.1007/s11663-022-02580-9

[28] X.L. Nie, Q. Xu, X. Xie, J.L. Li, Evolution behavior of oxide inclusions in Si–Mn deoxidized steel during billet heating process, Journal of Mining and Metallurgy, Section B: Metallurgy, 61 (1) (2025) 111–124. https://doi.org/10.2298/JMMB250109009N

[29] C. Liu, F. Ye, Mechanism on modification of MnO SiO_2–type oxide by interfacial solid–state reaction during heat treatment, Acta Metallurgica Sinica, 53 (1) (2017) 10–18. (in Chinese) https://doi.org/10.11900/0412.1961.2016.00120

[30] F. Ye, C. Liu, H. Ni, Q. Fang, X.Song, Influence of FeO on compound oxides in Si–Mn deoxidized steel during heat treatment at 1273 K, Iron and Steel, 53 (5) (2018) 39–44. (in Chinese) https://doi.org/10.13228/j.boyuan.issn0449-749x.20170457

MEĐUFAZNA INTERAKCIJA IZMEĐU KOMPLEKSNIH OKSIDA I MATRICE ČELIKA DEZOKSIDISANOG Si I Mn TOKOM TERMIČKE OBRADE

Xinlong Nie [a], Shannan Li [a], Qi Xu [a], Jianli Li [a,b,c,*]

[a] Ključna laboratorija za crnu metalurgiju i iskorišćenje resursa Ministarstva obrazovanja, Univerzitet za nauku i tehnologiju u Vuhanu, Vuhan, Hubei, Kina
[b] Pokrajinska ključna laboratorija Hubei za nove procese u proizvodnji gvožđa i čelika, Univerzitet za nauku i tehnologiju u Vuhanu, Vuhan, Hubei, Kina
[c] Državna ključna laboratorija za napredne vatrostalne materijale, Vuhan, Hubei, Kina

Apstrakt

Difuzioni parovi pripremljeni su u visokotemperaturnoj peći radi ispitivanja međupovršinskih reakcija između Si–Mn deoksidisanog čelika i oksidnih sistema CaO–SiO_2–Al_2O_3–MgO–MnO i CaO–SiO_2–Al_2O_3–MgO–MnO–FeO tokom termičke obrade na temperaturama od 1273, 1373 i 1473 K u trajanju od 10 sati. Sistematski su ispitani uticaji ovih reakcija na promenu hemijskog sastava i razvoj faza na međupovršini. Takođe je proučavan uticaj sadržaja FeO i različitih temperatura termičke obrade na ponašanje međupovršine između kompleksnih oksida i podloge od Si–Mn deoksidisanog čelika. Rezultati pokazuju da su, bez obzira na početni sadržaj FeO u oksidnoj fazi difuzionih parova, nakon termičke obrade u čeličnoj matrici nastali precipitati sastavljeni od SiO_2 i male količine MnO. U blizini međupovršine u oksidnoj fazi izdvojila se tamna faza sa visokim sadržajem SiO_2. Utvrđeno je da su širine zone osiromašene manganom (MDZ) i zone precipitacije čestica (PPZ) približno linearno povezane. U poređenju sa sistemom bez FeO, difuzioni parovi koji su sadržali 3 mas.% FeO pokazali su šire MDZ i PPZ zone u čeličnoj matrici nakon termičke obrade. Maksimalne širine i MDZ i PPZ zona zabeležene su nakon termičke obrade na 1373 K u trajanju od 10 sati.

Ključne reči: *Difuzioni par; Si–Mn deoksidisani čelik; Kompleksni oksid; Međupovršinska reakcija; Termička obrada*